Chemical Science

ROYAL SOCIETY OF CHEMISTRY

EDGE ARTICLE

View Article Online
View Journal | View Issue

Cite this: *Chem. Sci.*, 2025, **16**, 21624

All publication charges for this article have been paid for by the Royal Society of Chemistry

Received 18th August 2025
Accepted 9th October 2025

DOI: 10.1039/d5sc06297g

rsc.li/chemical-science

Unraveling the role of counter-cations in Pd-catalyzed carboxylic acid C–H activation

Zhewei Li,[a] Yanhui Tang[b] and Ming Lei *[a]

The counter-cation effect has been proved by experiments to be very crucial in the Pd-catalyzed C–H activation of carboxylic acid but its mechanism is still unclear. In this study, the reaction mechanism of the Pd-catalyzed mono-selective β-C(sp^3)–H heteroarylation of free carboxylic acids was investigated by the density functional theory (DFT) method and the role of the counter-cation effect in this reaction was unveiled. Different from the general understanding that dimeric or trimeric palladium species are the most stable forms, the calculated results indicate that dimeric palladium species tend to dissociate into monomers under the assistance of counter-cations, and then form more stable κ^1 coordination palladium species with carboxylic acids rather than κ^2 coordination palladium species. This enables the Pd center to activate the target C–H bond effectively and successfully. In the following C–C coupling process, the Pd–Ag–K catalytic model was proposed, which could drive the C(sp^3)–H (hetero)arylation of free carboxylic acids instead of the Pd–Ag synergistic model. The critical role of the base is to stabilize heterodimeric Pd(II)–Ag(I) species. Moreover, this model successfully explains the origin of the mono-selective β-C(sp^3)–H heteroarylation observed in experiments, in that the Pd(IV) species formed by the oxidative addition are too stable, thus preventing the reductive elimination in the second β-C(sp^3)–H heteroarylation.

Introduction

In the past decades, C–H bond functionalization has aroused tremendous interest among chemists and the activation and transformation of C–H bonds catalyzed by transition-metal (TM) complexes have opened up a new era in organic synthesis.[1–5] This strategy provides insights into new retro-synthetic disconnections, making it feasible for the late-stage functionalization of complex scaffolds.[6,7] However, a tremendous challenge in C–H functionalization is to realize diverse C(sp^3)–H functionalization of organic substrates bearing native functional groups such as carboxyl, carbonyl, amino and hydroxyl groups under mild conditions.[8–14] Palladium has emerged as one of the most effective catalysts in this field. Nevertheless, it is a significant challenge to realize Pd-catalyzed C(sp^3)–H activation directed by carboxylic acid due to the inherent weak coordination between Pd and carboxylic acid.[15] In addition, there are two coordination modes between Pd and carboxylic acid, κ^2 coordination and κ^1 coordination, while the expected active intermediates require a κ^1 coordination mode due to the geometric requirement of C–H bond activation (see Fig. 1a).[16] Unfortunately, the coordination mode of Pd with free carboxylic acid tends to adopt κ^2 coordination whether in its dimeric or monomeric structures. This coordination mode makes the metal center locked away from the C–H bonds, which leads to the target C–H bond being difficult to activate. In 2007, Yu *et al.* found that counter-cations could dramatically boost the reactivity of the Pd-catalyzed C–H activation of carboxylic acid.[17] They proposed that counter-cations could affect the coordination mode of Pd with carboxylic acid by interacting with carboxylate, thereby the Pd catalyst could bind in a favorable κ^1 manner for C–H activation, and prevent the formation of unreactive κ^2 Pd carboxylates (see Fig. 1b).[18] Since then, it has become widely accepted to use a base to promote Pd-catalyzed C–H activation of carboxylic acids or electron-deficient amides.[19] Recently, with the development of TM catalysts and bifunctional pyridone ligands (pyri-pyridine, pyri-sulfona, pyri-amide, pyri-imine), the C(sp^3)–H functionalization of free carboxylic acids has made milestone progress and enabled the previously elusive aliphatic C–H activation.[20–23] In 2021, Yu *et al.* developed two classes of pyridine-pyridone ligands that enabled the Pd-catalyzed dehydrogenative reactions of carboxylic acids to synthesize α,β-unsaturated carboxylic acids or γ-alkylidene butenolides.[24] Recently, our density functional theory (DFT) mechanistic investigation indicated that this reaction involves a cascade of catalytic species evolution from monomeric Pd species during C–H activation to heterodimeric Pd–Ag species during C–C coupling, and finally to homodimeric Ag–Ag species in the final cyclization step.[25] In 2023, Yu *et al.* reported the Pd-

[a]*State Key Laboratory of Chemical Resource Engineering, Institute of Computational Chemistry, College of Chemistry, Beijing University of Chemical Technology, Beijing 100029, China. E-mail: leim@mail.buct.edu.cn*

[b]*School of Materials Design and Engineering, Beijing Institute of Fashion Technology, Beijing, 100029, China*

catalyzed mono-selective β-C(sp^3)–H aza-heteroarylation of free aliphatic carboxylic acids (see Fig. 1c).[26] The key to the reaction is the utilization of bifunctional pyridone ligands, which could overcome the competitive coordination of heterocyclic nitrogen with the Pd center thus avoiding the formation of inactive Pd-heteroaryl intermediates. Aliphatic acids containing β-aza-heteroaryls with diverse quaternary carbon centers could be constructed by this synthetic strategy, which could provide a unique platform for the synthesis of many potential drug molecules. Although rapid progress has been made in experiments on Pd-catalyzed C(sp^3)–H activation directed by carboxylic acid substrates, the mechanism and the role of counter-cations in the reaction remain unclear.

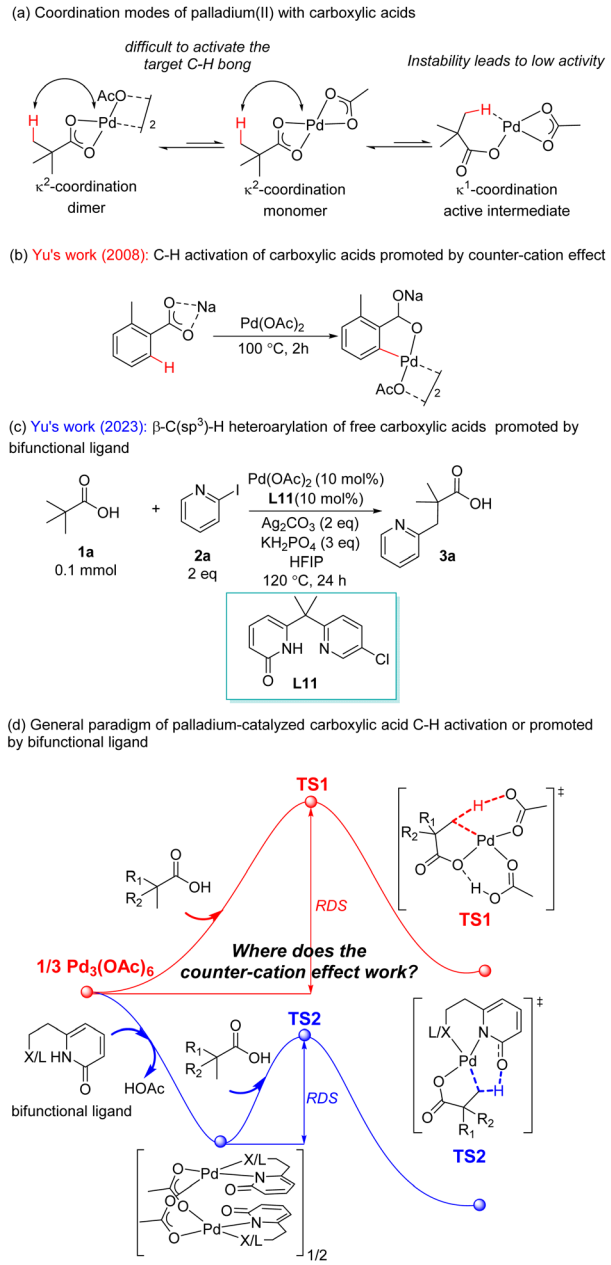

Fig. 1 The development of the Pd-catalyzed C–H activation of carboxylic acid.

Computational studies of Pd-catalyzed C–H activation directed by carboxylic acids are challenging due to the complexity of the experimental environment. A standard experimental environment usually requires Pd catalysts, ligands, substrates, bases, silver additives and solvents. In some cases, several silver additives and bases were used together, which involves various anions and cationic counterions.[27–29] Normally silver salts are regarded as terminal oxidants or merely as halide abstractors to abstract halides from intermediate palladacycles, and recent experimental and theoretical studies point out that Ag species could also form dimers with Pd to perform the crucial C–H activation process and the succeeding C–C coupling process.[30–33] In general, two computational model paradigms for Pd-catalyzed carboxylic acid C–H activation have been established corresponding to the reaction in the presence or absence of ligands, respectively (see Fig. 1d).[25,34] In the case without additional ligands, trimeric $Pd_3(OAc)_6$ could dissociate into monomeric $Pd(OAc)_2$, which could interact with the carboxylic acid/carboxylate substrate and release acetic acid/acetate. Then the C–H activation step occurs through the concerted metalation-deprotonation (CMD) mechanism *via* transition state **TS1**. The energy barrier for the rate-determining step (RDS) of the C–H activation process is the energy difference between **TS1** and $Pd_3(OAc)_6$. If additional ligands such as L,X-type bifunctional ligands are added, they will combine with $Pd_3(OAc)_6$ to form a more stable dimeric palladacyclic complex. The crystal structures of homodimeric palladium complexes have been obtained in experiments.[35] Similarly, the dimer could dissociate into monomers to realize the C–H activation process though the CMD mechanism *via* **TS2**.[25] The energy barrier of the RDS of the C–H activation process is the energy difference between **TS2** and homodimeric species. However, the role of the cationic counterion was not considered in the two computational models above for the Pd-catalyzed C–H activation directed by carboxylic acid because the participation of alkali metals has no effect on either side of the RDS. It should be noted that for X,X-type ligands such as the MPAA ligand or the pyridine ligand, the alkali metal moiety of carboxylate will be retained to satisfy charge balance requirements, thereby influencing the transition state and partially reflecting the counter-cation effect.[36,37] However, the counter-cation effect not only plays a role in the C–H activation of carboxylic acid catalyzed by Pd complexes promoted by the MPAA ligand, but is feasible in all cases. Moreover, the influence of counter-cations on the coordination mode of carboxylic acid with Pd is missed.

Inspired by the critical role of the counter-cation effect observed in experiments, which can significantly boost the system's reactivity in Pd-catalyzed C–H activation of carboxylic acids, the mechanism of the Pd-catalyzed C(sp^3)–H (hetero) arylation of free carboxylic acids has yet to be explored from a theoretical perspective. In this work the DFT method was employed to investigate the Pd-catalyzed mono-selective β-C(sp^3)–H heteroarylation of free carboxylic acids. The pivotal roles of the counter-cation effect, bases, and silver salts, as well as the origin of the excellent mono-selectivity, were unveiled.

Computational methods

In this study, the optimization of all geometric structures and frequency calculations of stationary points were performed at the PBE0-D3(BJ)/def2-SVP level using the Gaussian 09 program.[38–40] D3(BJ) denotes the Grimme's dispersion interaction correction method.[41] The solvent effect of HFIP ($\varepsilon = 16.7$) was simulated by the SMD continuum solvent model in the calculation.[42] Frequency analysis was conducted to verify that the stationary points correspond to either minima (zero imaginary frequencies) or transition states (only one imaginary frequency). The improved elastic image pair (i-EIP) method was used for finding transition states integrating with the Gaussian 09 program.[43,44] Intrinsic reaction coordinates (IRC) calculations were performed to confirm intermediates along reaction pathways.[45] Additionally, single point calculations were computed using the ORCA package to obtain better electronic energy with the ωB97M-V functional and def2-TZVPP basis set, based on optimized geometries at the PBE0-D3(BJ)/def2-SVP level.[46–48] For the key stationary points, other possible conformations were searched by adjusting the coordination mode between ligands and metal centers; only the most favorable ones were reported (see Table S1 in the SI). All energies discussed in the following parts are Gibbs free energies calculated at 298.15 K unless otherwise stated. A correction factor of 1.89 kcal mol^{-1} was applied for the standard state change from 1.0 atm to 1.0 M.[49] Computed geometric structures are illustrated using CYLView1.0.[50] Energies and Cartesian coordinates of all optimized structures are given in the SI.

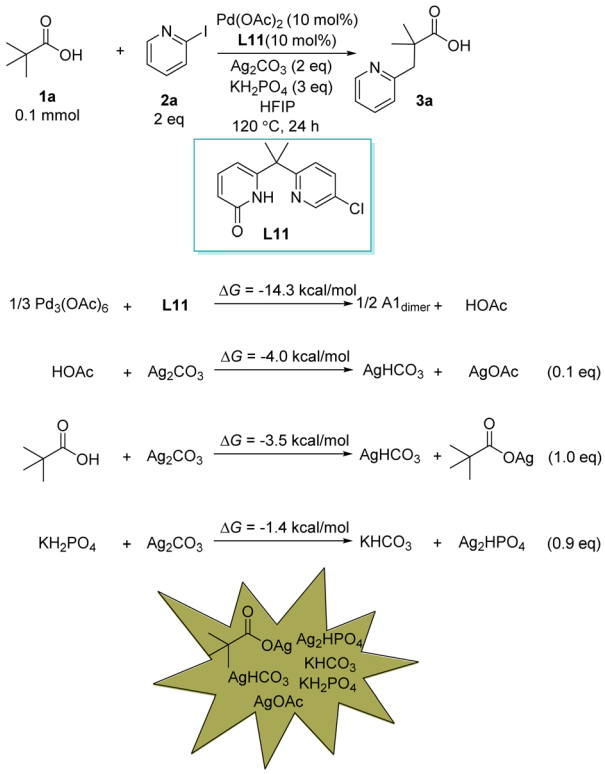

Fig. 3 The formation of six possible bases and silver salt species in the initial stage of Pd-catalyzed heteroarylation of carboxylic acids.

Results and discussion

The Pd-catalyzed mono-selective β-C(sp^3)–H heteroarylation of free carboxylic acids consists of two processes: the C(sp^3)–H activation process and the C–C coupling process. As shown in Fig. 2, in the C(sp^3)–H activation process, the five-membered palladacyclic intermediate is formed and the cationic counterion such as K^+ and Ag^+ could facilitate this process. Then the C–C coupling process is completed *via* the interaction of the palladacyclic intermediate and iodopyridine substrate. Interestingly, the six-membered chelating ligand **L11** could only promote the mono-selective β-C(sp^3)–H heteroarylation of free carboxylic acids instead of the second β-C(sp^3)–H heteroarylation in the reported experiment,[26] implying that the second heteroarylation could be prevented.

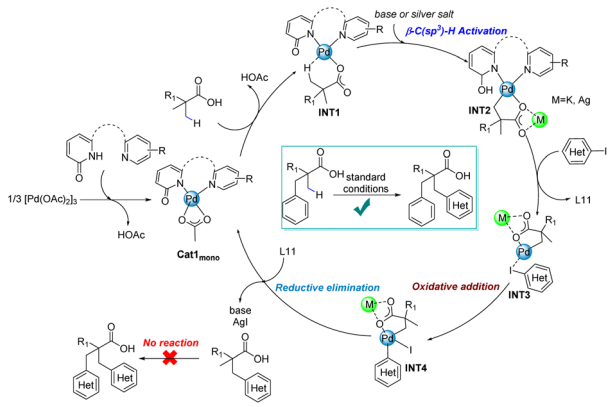

Fig. 2 The catalytic cycle of the Pd-catalyzed mono-selective β-C(sp^3)–H heteroarylation of free carboxylic acids.

Possible base and silver salt species in the reaction

The possible bases and silver salts in the Pd-catalyzed heteroarylation of carboxylic acids with iodopyridines were investigated at first. In the reaction, two equivalents of Ag_2CO_3 and three equivalents of KH_2PO_4 were initially added, and they were mixed with palladium acetate, pyridine-pyridone ligand **L11** and pivalic acid **1a** to form various possible species. As shown in Fig. 3, the calculated results show that the formation of $\mathbf{A1_{dimer}}$ resulting from the combination of pre-catalyst $Pd(OAc)_2$ and **L11** is exergonic by 14.3 kcal mol^{-1}. Subsequently, both the acetic acid and the pivalic acid could react with Ag_2CO_3 to generate $AgHCO_3$, AgOAc and *t*BuCOOAg. Finally, the excess Ag_2CO_3 will be consumed by KH_2PO_4 to form Ag_2HPO_4 and $KHCO_3$, which is exergonic by 1.4 kcal mol^{-1}. Therefore, six possible base and silver salt species ($AgHCO_3$ (1.1 eq.), AgOAc (0.1 eq.), *t*BuCOOAg (1.0 eq.), Ag_2HPO_4 (0.9 eq.), $KHCO_3$ (0.9 eq.) KH_2PO_4 (2.1 eq.)) might assist the succeeding C–H activation process (see Fig. S1 in the SI for thermodynamically processes of other unfavorable possible bases such as KOAc and *t*BuCOOK).

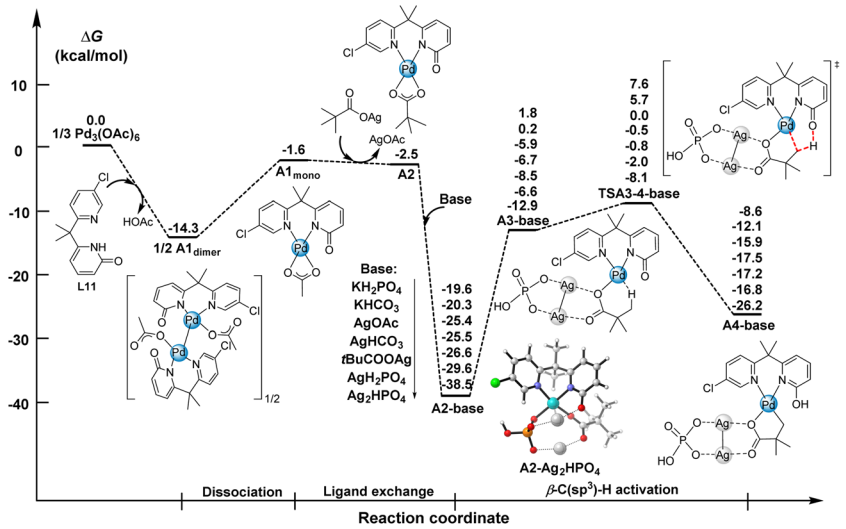

Fig. 4 The Gibbs energy profiles (in kcal mol^{-1}) of Pd-catalyzed β-C(sp^3)–H activation of pivalic acids promoted by the counter-cation effect.

β-C(sp^3)–H activation of pivalic acids catalyzed by Pd complexes

Then the mechanism of the Pd-catalyzed β-C(sp^3)–H activation of pivalic acids promoted by six-membered chelating ligand **L11** was investigated. As shown in Fig. 4, the dimeric palladacyclic complex $\mathbf{A1_{dimer}}$ dissociates into the monomeric $\mathbf{A1_{mono}}$, which is endergonic by 12.7 kcal mol^{-1}. Then the AcO$^-$ anionic moiety of $\mathbf{A1_{mono}}$ was replaced by *t*BuCOO$^-$ aided by the Ag(I) cation to form **A2**. In the previous calculated models, the coordination mode of Pd and carboxylic acid will change from a κ^2 manner into a κ^1 manner due to geometric requirements of the following C–H activation step.[25] However, the counter-cation effect in those models was completely ignored. Inspired by the experimental hypothesis that the counter-cations could affect the coordination mode of Pd with carboxylic acids by interacting with the carboxylate,[51] the Pd-catalyzed C–H activation of carboxylic acid promoted by bases and silver salts was studied, and a more stable structure, **A2-base** (base represents an inorganic base or silver salt) formed by **A2** with these promoters was located. The interaction models of seven bases or silver salts with **A2** were systemically investigated (AgH_2PO_4 was also considered because it could be produced as the reaction proceeds, see Fig. S2 in the SI). Among them, the combination of Ag_2HPO_4 and **A2** is the most stable theoretically, which is exergonic by 36.0 kcal mol^{-1}. Several possible coordination modes of $\mathbf{A2\text{-}Ag_2HPO_4}$ were adopted, and the most favorable conformation has the *cis* arrangement of the *t*BuCOO$^-$ anionic moiety and the nitrogen of pyridine (see Fig. S3 in the SI). The coordination modes of the other six **A2-base** intermediates were also investigated, and the most favorable coordination mode is similar to that of $\mathbf{A2\text{-}Ag_2HPO_4}$. Subsequently, the alkali or silver metals continue to interact with the carboxylic acid moieties of the **A2-base**, allowing it to isomerize into a more reactive intermediate, the **A3-base**, which features an agostic C–H···Pd interaction. Despite this process being endergonic, the Pd center of the **A3-base** could engage with the β-C(sp^3)–H bond, which could weaken the target C–H bond of the **A3-base** and facilitate the ensuing C–H activation step. In the C–H activation step, the oxygen of the 2-pyridone moiety of the **L11** ligand acts as an intramolecular base to deprotonate the methyl C–H bond *via* the **TSA3-4-base** to form a five-membered palladacyclic intermediate **A4-base** (CMD mechanism). Among the β-C(sp^3)–H activation processes promoted by seven bases mentioned above, although the energy barrier of the C–H activation step promoted by Ag_2HPO_4 is the highest ($\Delta G^{\ddagger}$ = 30.4 kcal mol^{-1}), the $\mathbf{A2\text{-}Ag_2HPO_4}$ intermediate is the most stable in energy compared to the other six **A2-base** intermediates, and the relative free energy of transition state $\mathbf{TSA3\text{-}4\text{-}Ag_2HPO_4}$ is the lowest among all transition states of the C–H activation promoted by bases or silver salts. Therefore, the C–H activation promoted by Ag_2HPO_4 is proposed to be more favorable than that promoted by other bases or silver salts. This agrees well with experiments reported by Yu *et al.*,[26] in which the yields of the reaction are 71% at 120 °C and 12% at 100 °C for 24 hours. This implies that the energy barrier of the reaction is relatively high.

On the other hand, the mechanism of Pd-catalyzed β-C(sp^3)–H heteroarylation was also investigated in the absence of bases and silver salts (see Fig. S6 in the SI). The energy barrier for C–H activation is 27.5 kcal mol^{-1}, which is lower than that promoted by Ag_2HPO_4 ($\Delta G^{\ddagger}$ = 30.4 kcal mol^{-1}), but higher than that promoted by other bases or silver salts mentioned above ($\Delta G^{\ddagger}$ = 25.0 ~ 27.2 kcal mol^{-1}). An experimental report by Maiti *et al.* also showed that Pd could achieve the C–H activation of pivalic acids to form a five-membered palladacyclic intermediate in the absence of counter-cations.[52] Therefore, not all bases or silver salts are beneficial to the C–H activation of carboxylic acid, which explains that different silver salts or bases are needed in different experiments and why the influence of counter-cations was not considered in previous theoretical research. However, bases or silver salts are necessary because of the requirement of the subsequent C–H functionalization process (the calculated

energy barrier for the following C–C coupling step is 41.9 kcal mol^{-1} in the absence of bases and silver salts in the study). In general, the interaction of alkali or silver metals with the carboxylic acid moieties of the **A2-base** is of importance and in the **A2-base**, Pd and Ag/K coordinate with the two oxygen atoms of the substrate carboxylic acid respectively, which supports the experimental hypothesis that alkali metals coordinate with the carboxylic acid, thus preventing the κ^2 coordination of Pd with the carboxylic acid, so that the Pd could bind in a favorable κ^1 manner for C–H activation. In a word, the counter-cation effect is beneficial to the depolymerization process and the coordination inversion of the carboxylic acid with the Pd center from κ^2 to κ^1. It should be noted that not all bases or silver salts could promote the C–H activation step of carboxylic acids.

C–C coupling catalyzed by Pd(II)–Ag(I)–K species

Following the C–H activation process, the C–C coupling process of the palladacyclic species **A4-base** with iodopyridine occurs. It is still unclear whether bases and silver salts participate in the C–C coupling process or not. In the C–H activation process mentioned above, the Pd-catalyzed β-C(sp^3)–H activation proceeding *via* the CMD mode and promoted by Ag_2HPO_4 should be the most advantageous pathway in the reaction. In this context, silver acts not as a transition metal, but more like an alkali metal, functioning as a counter-cation. Thus it can be reasonably speculated that both alkali metals and silver salts could promote the C–H activation step of carboxylic acids independently.

As shown in Fig. 5, three possible reaction pathways (pathways I, II and III) for the C–C coupling process of the palladacyclic intermediate **A4-Ag$_2$HPO$_4$** were investigated. Pathway I denotes C–C coupling in the absence of the base KH_2PO_4, which involves oxidative addition and reductive elimination *via* **A5-Ag** to realize a heterodimeric Pd–Ag cooperative catalysis. Pathway II denotes the pathway in the absence of the silver salt AgH_2PO_4, which involves the Pd-catalyzed cross-coupling reaction of iodopyridine with a carboxylic acid assisted by a base. Pathway III denotes the C–C coupling process realized by Pd–Ag–K species **A5**. The calculated results show that the energy barriers of pathways I and II are too high to happen, this might be due to the stability of the palladacyclic intermediate **A4-Ag$_2$HPO$_4$**. In contrast, pathway III is favorable compared to pathways I and II based on corresponding Gibbs energy profiles (see Fig. S7 and S8 in the SI). Fig. 6 presents free energy profiles of the C–C coupling process catalyzed by Pd–Ag–K species along pathway III. Along pathway III the intermediate **A4-Ag$_2$HPO$_4$** interacts with one KH_2PO_4 molecule and one iodopyridine molecule while releases one **L11-Ag** molecule to form intermediate **A5** with a key Pd–Ag–K cooperative catalytic structure. The formation of **A5** from **A4-Ag$_2$HPO$_4$** is exergonic by 2.2 kcal mol^{-1}. In the following oxidative addition, the iodopyridine substrate coordinates with the Pd(II) center of **A5** to form Pd(IV) species **A6** *via* **TSA5-6** with an energy barrier of 18.9 kcal mol^{-1}. Then C–C coupling occurs easily *via* **TSA6-7** from **A6** to **A7** in the reductive elimination step. The energy barrier for this step is 9.0 kcal mol^{-1}. Finally, **A7** undergoes ligand exchange to regenerate the catalytic species **A2-Ag$_2$HPO$_4$**, releasing the heteroarylation product and completing the whole catalytic cycle.

In the Pd-catalyzed mono-selective β-C(sp^3)–H heteroarylation of free carboxylic acids, the calculated results show that the C(sp^3)–H bond activation step from **A2-Ag$_2$HPO$_4$** to **TSA3-4-Ag$_2$HPO$_4$** is the rate-determining step, with an energy barrier of 30.4 kcal mol^{-1}. The succeeding C–C coupling process is catalyzed by the Pd–Ag–K species along reaction pathway III. In this model, the role of silver is not only to abstract halides as halide abstractors, but also to assist the oxidative addition and the reductive elimination processes by forming the heterodimeric Pd(II)–Ag(I) species. Remarkably, Pd will form a stable palladacyclic intermediate with counter-cations in the C–H activation process of free carboxylic acids due to the counter-cation effect. The stability of the intermediate such as **A4-base** results in Pd–Ag model losing the catalytic activity for the subsequent C–C coupling process. Therefore, the role of the

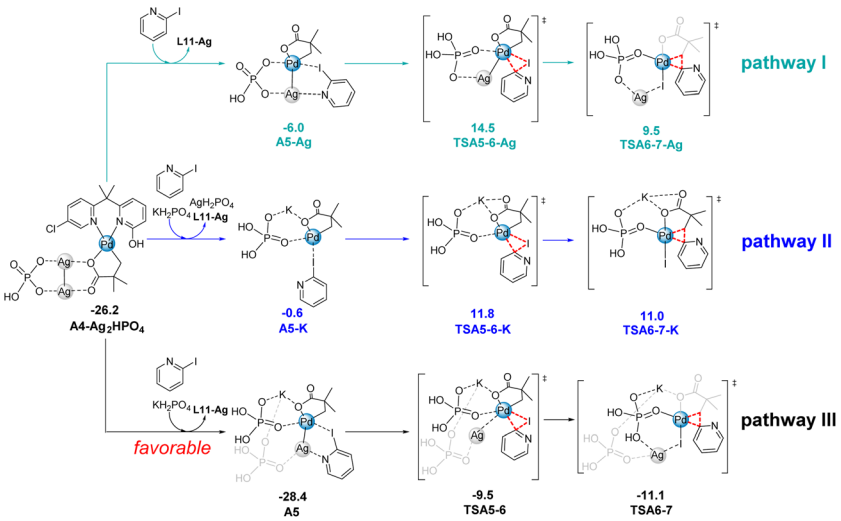

Fig. 5 Three possible pathways for the C–C coupling process from A4-Ag_2HPO_4.

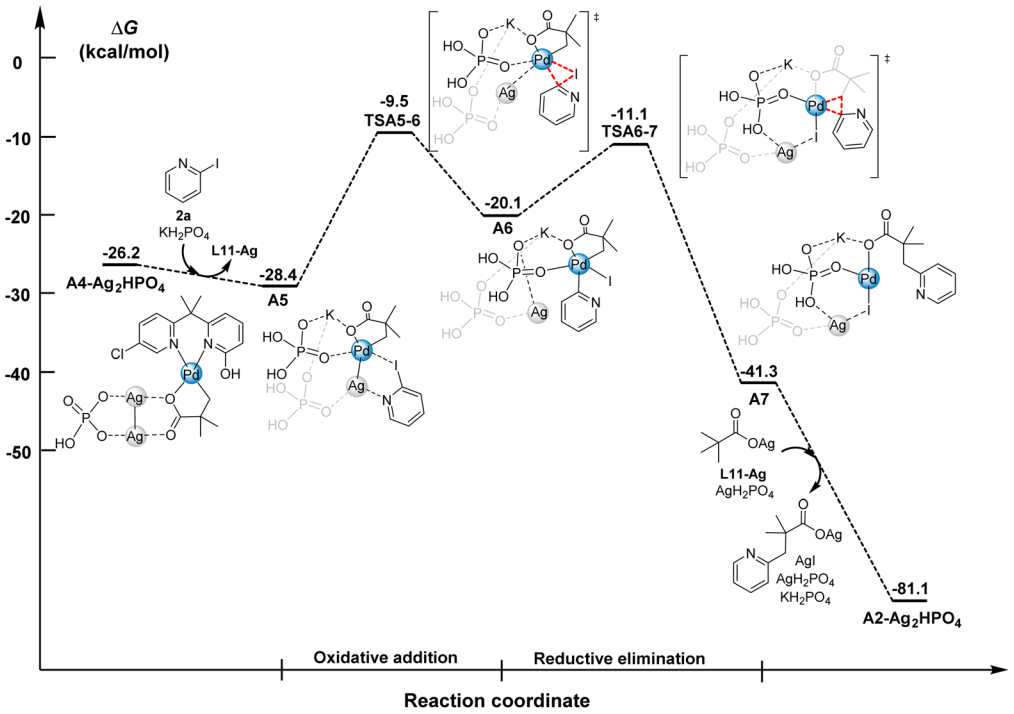

Fig. 6 The Gibbs energy profiles (in kcal mol^{-1}) of the C–C coupling process catalyzed by Pd–Ag–K species along pathway III.

base is to stabilize heterodimeric Pd(II)–Ag(I) species and thereby drive the following C–C coupling process. Schaefer and Sunoj *et al.* also pointed out the electrostatic stabilization of additive CsF for the Pd(II)–Ag(I) species in the Pd-catalyzed aryl amination reaction.[53] Herein the proposed Pd–Ag–K model unveils the role of bases and silver salts in the Pd-catalyzed C(sp^3)–H (hetero)arylation of free carboxylic acids theoretically.

Moreover, in reported experimental studies of the Pd-catalyzed dehydrogenation of aliphatic acids, the C–H activation process could proceed normally in the absence of alkali metals or silver salts.[24,54,55] In 2024 Jiao *et al.* reported the Pd-catalyzed enantioselective C(sp^3)–H functionalization reaction, and obtained the crystal structure of key palladacyclic intermediates by adding Ag_2O in the absence of alkali metals.[56] It could be seen that in the C–H activation process of carboxylic acid, the roles of the alkali metal and silver salt are similar, both provide cations as cationic counterions (note that silver salts could also be used as terminal oxidants). Nevertheless, bases and silver salts are necessary in this reaction,[26] implying that both base and silver salt species play a pivotal role in the subsequent C–C coupling process. Therefore, the proposed Pd–Ag–K model is also supported by experiments.

Origin of mono-selective β-C(sp^3)–H heteroarylation

Meanwhile, the origin of the experimentally observed mono-selective β-C(sp^3)–H heteroarylation of carboxylic acids was also investigated. Based on the theoretical results on the reaction mechanism of the first β-C(sp^3)–H heteroarylation above, the C–H activation process is proposed to be the rate-determining step while the latter C–C coupling process occurs easier than the former. The second β-C(sp^3)–H heteroarylation will adopt a similar C–H activation mode to the first one (see more details in Fig. S9 of the SI). Then the second C–C coupling process catalyzed by the proposed Pd–Ag–K model along pathway III was studied. As shown in Fig. 7, the palladacyclic intermediate **A11** combines with one molecule KH_2PO_4 and one molecule iodopyridine while releasing one molecule **L11-Ag** to form intermediate **A12**, which is endergonic by 0.2 kcal mol^{-1}. In the second oxidative addition step, the iodopyridine substrate coordinates with the Pd(II) center *via* **TSA12-13** to form Pd(IV) species **A13** with an energy barrier of 13.8 kcal mol^{-1}. Different from the Pd(IV) species **A6** in the first C–C coupling process, **A13** is very stable due to the coordination of extra pyridine groups with Pd(IV) center. **A13** could isomerize into **A13-a**, and then the second C–C reductive elimination step occurs. The energy barrier for this step is 32.7 kcal mol^{-1} from **A13** to **A14** *via* **TSA13-14**. In the first C–C coupling process, the first oxidative addition step is more difficult than the first reductive elimination step. However, in the second C–C coupling process, the reductive elimination step becomes the most difficult one in the whole reaction. For the stationary points along pathway III of the second C–C coupling process, possible conformations by adjusting the coordination modes between ligands and metal centers were thoroughly searched to ensure the reliability of the preferable structures of stationary points presented in Fig. 7 (see Fig. S10–S12 of the SI). The calculated results indicate that the most stable conformation of transition state **TSA13-14** of the reductive elimination step does not involve the coordination of pyridine with the Pd(IV) center, and that the second β-C(sp^3)–H heteroarylation of the reaction is inhibited due to the excessive stability of the intermediate

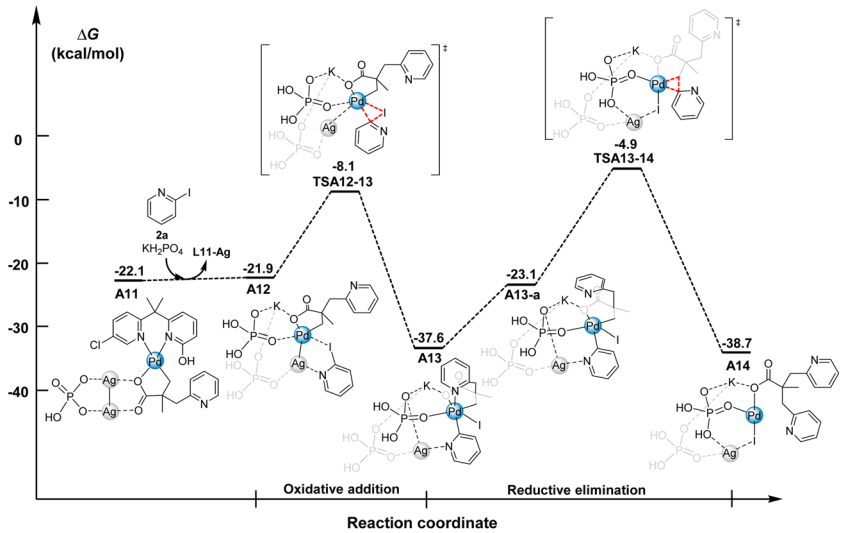

Fig. 7 The Gibbs energy profiles (in kcal mol^{-1}) of the second C–C coupling process catalyzed by Pd–Ag–K species along pathway III.

A13. This agrees with the experimentally observed mono-selective heteroarylation of carboxylic acids and further elucidates the reasonability of the proposed Pd–Ag–K model in this study. In addition, the original experimental report also showed excellent mono-selective heteroarylation when 4-iodopyridines were used as substrates. In this case, intermediate A13 couldn't be formed. The calculated results showed that the energy barrier is 31.3 kcal mol^{-1} for the second β-C(sp^3)–H activation step and is 35.4 kcal mol^{-1} for the second reductive elimination step, thus preventing the second heteroarylation process (see more details and descriptions in Fig. S13 and S14 of the SI). This might be due to that the nitrogen atom at the *para*-position having more electron donating ability makes the second reductive elimination step more difficult.

Conclusions

In summary, the counter-cation effect and the reaction mechanism of the Pd-catalyzed mono-selective β-C(sp^3)–H heteroarylation of carboxylic acids were investigated using the DFT method, and the pivotal roles of the ligands, silver additives and bases in this reaction were also unveiled. Different from the general understanding that the dimeric or trimeric palladium species are the most stable forms, the calculated results indicate that the dimeric palladium species tend to dissociate into monomers under the assistance of counter-cations and then form a more stable κ^1 coordination species with carboxylic acid. This change from κ^2 to κ^1 coordination mode of carboxylic acid with Pd enables the Pd center to effectively interact with the target C–H bond, thus facilitating the succeeding C–H activation. The calculated results indicated that not all bases or silver salts are beneficial to the C–H activation of the carboxylic acids. Meanwhile, the pivotal role of bases and silver salts in the subsequent C–C coupling process was revealed and a Pd–Ag–K model was proposed. In this model, silver salt acts as a halide abstractor and could promote the oxidative addition and the reductive elimination of the C–C coupling process by forming heterodimeric Pd(II)–Ag(I) species, while the base is to stabilize the heterodimeric Pd(II)–Ag(I) species by forming a Pd–Ag–K structure. Finally, the origin of the mono-selective β-C(sp^3)–H heteroarylation of the reaction could be elucidated based on the Pd–Ag–K model, in which the Pd(IV) species formed in the oxidative addition are too stable to undergo the following reductive elimination in the second β-C(sp^3)–H heteroarylation. This work could provide important theoretical insights into the role of silver salts and bases in Pd-catalyzed carboxylic acid C–H activation.

Author contributions

Ming Lei and Zhewei Li designed this work, Zhewei Li performed the DFT calculations, Zhewei Li, Yanhui Tang and Ming Lei co-wrote the manuscript, Ming Lei supervised the whole research. All of the authors discussed and commented on the manuscript.

Conflicts of interest

The authors declare no competing financial interest.

Data availability

The data supporting this article have been included as part of the supplementary information (SI).

Supplementary information: computational details, relative free energies and atomic coordinates of all optimized structures (*XYZ*). See DOI: **https://doi.org/10.1039/d5sc06297g**.

Acknowledgements

This work was supported by the National Natural Science Foundation of China (Grant No. 22473008, 22411530047) and Beijing Municipal Natural Science Foundation (Grant No.

2242014). We also thank the High Performance Computing (HPC) Platform at Beijing University of Chemical Technology (BUCT) for providing part of the computational resources.

Notes and references

1 J. H. Docherty, T. M. Lister, G. McArthur, M. T. Findlay, P. Domingo-Legarda, J. Kenyon, S. Choudhary and I. Larrosa, *Chem. Rev.*, 2023, **123**, 7692–7760.
2 S. K. Sinha, S. Guin, S. Maiti, J. P. Biswas, S. Porey and D. Maiti, *Chem. Rev.*, 2022, **122**, 5682–5841.
3 B. Liu, A. M. Romine, C. Z. Rubel, K. M. Engle and B. F. Shi, *Chem. Rev.*, 2021, **121**, 14957–15074.
4 B. S. Yeqiang Han, *Acta Chim. Sin.*, 2023, **81**, 1522–1540.
5 O. Baudoin, *Chem. Soc. Rev.*, 2011, **40**, 4902–4911.
6 L. Guillemard, N. Kaplaneris, L. Ackermann and M. J. Johansson, *Nat. Rev. Chem.*, 2021, **5**, 522–545.
7 A. Uttry, S. Mal and M. van Gemmeren, *J. Am. Chem. Soc.*, 2021, **143**, 10895–10901.
8 T. Sheng, T. Zhang, Z. Zhuang and J.-Q. Yu, *Nat. Synth.*, 2024, **3**, 1550–1559.
9 D. A. Strassfeld, C. Y. Chen, H. S. Park, D. Q. Phan and J. Q. Yu, *Nature*, 2023, **622**, 80–86.
10 Y. H. Li, N. Chekshin, Y. Lu and J. Q. Yu, *Nature*, 2025, **637**, 608–614.
11 Z. Li and J.-Q. Yu, *J. Am. Chem. Soc.*, 2023, **145**, 25948–25953.
12 K. M. Engle, T. S. Mei, M. Wasa and J. Q. Yu, *Acc. Chem. Res.*, 2012, **45**, 788–802.
13 F. Ghiringhelli, A. Uttry, K. K. Ghosh and M. van Gemmeren, *Angew. Chem., Int. Ed.*, 2020, **59**, 23127–23131.
14 Q. Zhang and B.-F. Shi, *Acc. Chem. Res.*, 2021, **54**, 2750–2763.
15 E. L. Lucas, N. Y. S. Lam, Z. Zhuang, H. S. S. Chan, D. A. Strassfeld and J. Q. Yu, *Acc. Chem. Res.*, 2022, **55**, 537–550.
16 J. He, M. Wasa, K. S. L. Chan, Q. Shao and J.-Q. Yu, *Chem. Rev.*, 2017, **117**, 8754–8786.
17 R. Giri, N. Maugel, J. J. Li, D. H. Wang, S. P. Breazzano, L. B. Saunders and J. Q. Yu, *J. Am. Chem. Soc.*, 2007, **1299**, 3510–3511.
18 R. Giri and J. Q. Yu, *J. Am. Chem. Soc.*, 2008, **130**, 14082–14083.
19 D. Li, X.-B. He, L. Jin, X. Yu and Q. Zhang, *Tetrahedron Lett.*, 2024, 138.
20 K. Wu, N. Lam, D. A. Strassfeld, Z. Fan, J. X. Qiao, T. Liu, D. Stamos and J. Q. Yu, *Angew. Chem., Int. Ed.*, 2024, **63**, e202400509.
21 T. Zhang, Z.-Y. Zhang, G. Kang, T. Sheng, J.-L. Yan, Y.-B. Yang, Y. Ouyang and J.-Q. Yu, *Science*, 2024, **384**, 793–798.
22 J.-M. Yang, Y.-K. Lin, T. Sheng, L. Hu, X.-P. Cai and J.-Q. Yu, *Science*, 2023, **380**, 639–644.
23 Q. Shao, K. Wu, Z. Zhuang, S. Qian and J. Q. Yu, *Acc. Chem. Res.*, 2020, **53**, 833–851.
24 Z. Wang, L. Hu, N. Chekshin, Z. Zhuang, S. Qian, J. X. Qiao and J.-Q. Yu, *Science*, 2021, **374**, 1281–1285.
25 Z. Li, Y. Tang and M. Lei, *ACS Catal.*, 2024, **14**, 14263–14273.
26 G. Meng, L. Hu, M. Tomanik and J. Q. Yu, *Angew. Chem., Int. Ed.*, 2023, **62**, e202214459.
27 J. L. Yan, L. Hu, Y. Lu and J. Q. Yu, *J. Am. Chem. Soc.*, 2024, **146**, 29311–29314.
28 H. S. S. Chan, J.-M. Yang and J.-Q. Yu, *Science*, 2022, **376**, 1481–1487.
29 Z. Zhuang, A. N. Herron, S. Liu and J. Q. Yu, *J. Am. Chem. Soc.*, 2021, **143**, 687–692.
30 M. Anand, R. B. Sunoj and H. F. Schaefer 3rd, *J. Am. Chem. Soc.*, 2014, **136**, 5535–5538.
31 Y. F. Yang, G. Chen, X. Hong, J. Q. Yu and K. N. Houk, *J. Am. Chem. Soc.*, 2017, **139**, 8514–8521.
32 W. Feng, T. Wang, D. Liu, X. Wang and Y. Dang, *ACS Catal.*, 2019, **9**, 6672–6680.
33 T. Bhattacharya, S. Dutta and D. Maiti, *ACS Catal.*, 2021, **11**, 9702–9714.
34 H.-M. Shan, Q. Wang, Z.-H. Sun, Y. Bu and L.-P. Xu, *Org. Chem. Front.*, 2024, **11**, 6135–6143.
35 Z. Li, Z. Wang, N. Chekshin, S. Qian, J. X. Qiao, P. T. Cheng, K.-S. Yeung, W. R. Ewing and J.-Q. Yu, *Science*, 2021, **372**, 1452–1457.
36 L.-P. Xu, Z. Zhuang, S. Qian, J.-Q. Yu and D. G. Musaev, *ACS Catal.*, 2022, **12**, 4848–4858.
37 B. F. Shi, N. Maugel, Y. H. Zhang and J. Q. Yu, *Angew. Chem., Int. Ed.*, 2008, **47**, 4882–4886.
38 C. Adamo and V. Barone, *J. Chem. Phys.*, 1999, **110**, 6158–6170.
39 F. Weigend and R. Ahlrichs, *Phys. Chem. Chem. Phys.*, 2005, **7**, 3297–3305.
40 M. J. Frisch, G. W. Trucks, H. B. Schlegel, G. E. Scuseria, M. A. Robb, J. R. Cheeseman, G. Scalmani, V. Barone, B. Mennucci, G. A. Petersson, H. Nakatsuji, M. Caricato, X. Li, H. P. Hratchian, A. F. Izmaylov, J. Bloino, G. Zheng, J. L. Sonnenberg, M. Hada, M. Ehara, K. Toyota, R. Fukuda, J. Hasegawa, M. Ishida, T. Nakajima, Y. Honda, O. Kitao, H. Nakai, T. Vreven, J. A. Montgomery Jr, J. E. Peralta, F. Ogliaro, M. Bearpark, J. J. Heyd, E. Brothers, K. N. Kudin, V. N. Staroverov, T. Keith, R. Kobayashi, J. Normand, K. Raghavachari, A. Rendell, J. C. Burant, S. S. Iyengar, J. Tomasi, M. Cossi, N. Rega, J. M. Millam, M. Klene, J. E. Knox, J. B. Cross, V. Bakken, C. Adamo, J. Jaramillo, R. Gomperts, R. E. Stratmann, O. Yazyev, A. J. Austin, R. Cammi, C. Pomelli, J. W. Ochterski, R. L. Martin, K. Morokuma, V. G. Zakrzewski, G. A. Voth, P. Salvador, J. J. Dannenberg, S. Dapprich, A. D. Daniels, O. Farkas, J. B. Foresman, J. V. Ortiz, J. Cioslowski and D. J. Fox, *Gaussian 09, Rev. D. 01*, Gaussian, Inc, Wallingford, CT, 2013.
41 S. Grimme, J. Antony, S. Ehrlich and H. Krieg, *J. Chem. Phys.*, 2010, **132**, 154104.
42 A. V. Marenich, C. J. Cramer and D. G. Truhlar, *J. Phys. Chem. B*, 2009, **113**, 6378–6396.
43 Y. Liu, H. Qi and M. Lei, *J. Chem. Theory Comput.*, 2022, **18**, 5108–5115.
44 Y. Liu, H. Qi and M. Lei, *J. Chem. Theory Comput.*, 2023, **19**, 2410–2417.

45 H. P. Hratchian and H. B. Schlegel, *J. Chem. Phys.*, 2004, **120**, 9918–9924.
46 F. Neese, F. Wennmohs, U. Becker and C. Riplinger, *J. Chem. Phys.*, 2020, **152**, 224108.
47 F. Neese, *Wiley Interdiscip. Rev.: Comput. Mol. Sci.*, 2022, **12**, e1606.
48 N. Mardirossian and M. Head-Gordon, *J. Chem. Phys.*, 2016, **144**, 214110.
49 V. S. Bryantsev, M. S. Diallo and W. A. Goddard, *J. Phys. Chem. B*, 2008, **112**, 9709–9719.
50 C. Y. Legault, *CYLview, 1.0b*, Universite de Sherbrooke, 2009, **http://www.cylview.org**.
51 X. Chen, K. M. Engle, D. H. Wang and J. Q. Yu, *Angew. Chem., Int. Ed.*, 2009, **48**, 5094–5115.
52 P. Dolui, J. Das, H. B. Chandrashekar, S. S. Anjana and D. Maiti, *Angew. Chem., Int. Ed.*, 2019, **58**, 13773–13777.
53 M. Anand, R. B. Sunoj and H. F. Schaefer, *ACS Catal.*, 2015, **6**, 696–708.
54 T. Sheng, G. Kang, Z. Zhuang, N. Chekshin, Z. Wang, L. Hu and J. Q. Yu, *J. Am. Chem. Soc.*, 2023, **145**, 20951–20958.
55 T. Sheng, Z. Zhuang, Z. Wang, L. Hu, A. N. Herron, J. X. Qiao and J. Q. Yu, *J. Am. Chem. Soc.*, 2022, **144**, 12924–12933.
56 C. H. Yuan, X. X. Wang, K. Huang and L. Jiao, *Angew. Chem., Int. Ed.*, 2024, **63**, e202405062.